Conference Paper, Published Version

Radecki-Pawlik, Artur; Plesinski, Karol; Wyzga, Bartolomiej

Analysis of Chosen Hydraulic Parameters of a Rapid Hydraulic Structure (RHS) in Porebianka Stream

IWLHS, 20-22/02/2013, Aachen - Bung & Pagliara (eds) - © 2013 Bundesanstalt für Wasserbau ISBN 978-3-939230-04-5

Analysis of Chosen Hydraulic Parameters of a Rapid Hydraulic Structure (RHS) in Porębianka Stream, Polish Carpathians

A. Radecki-Pawlik & K. Plesiński
New Department of Hydraulic Engineering and Geotechnique
University of Agriculture in Kraków, Poland

B. Wyżga
Institute of Nature Conservation, Polish Academy of Sciences, Kraków, Poland

ABSTRACT: Application of grade correction of a channel using rapid hydraulic structures (RHS) is a new tendency in modern river training. These structures meet both technical and ecological requirements. They decrease the longitudinal slope of the stream, differentiate the flow regime and dynamics, recreate the braided pattern of the channel and do not stop the migration of fish and macroinvertebrates. Moreover, they mimic a pool and riffle channel morphology and thus conform with the requirements of the Water Framework Directive of the EU. In this paper, we analyse chosen hydraulic parameters of a rapid hydraulic structure constructed in a gravel-bed Porębianka Stream, Polish Carpathians.

Keywords: rapid hydraulic structure (RHS), hydrodynamic parameters, shear stress, velocity

1 INTRODUCTION

Pool and riffle morphology is one of a few channel pattern types found in mountain watercourses (Montgomery, Buffington 1997) and the one typical of inhabited, lower sections of mountain and piedmont valleys. Pool-riffle sequences occur with an average spacing of five to seven times the channel width (Gregory et al. 1994) and the regular downstream variability in bed morphology is associated with that in bed-material size, with coarser material forming the bed on riffles than in pools (Keller 1971, Milne 1982). According to the velocity reversal hypothesis (Keller 1971), the areal sorting of bed material in pool-riffle sequences reflects different patterns of flow velocity at discharges lower and higher than bankfull. Further studies confirmed the hypothesis, indicating that not only the zones of different velocity but also those of bed shear stress and unit stream power in pool-riffle sequences reverse as flow increases (e.g. Teisseyre 1984, Radecki-Pawlik 2002). The differentiation of channel bed into pools and riffles exerts a remarkable influence on physical and biotic patterns in mountain river channels. Areas with different hydrodynamic conditions along pool-riffle sequences provide habitats for varied benthic invertebrate communities (Pastuchová et al. 2008), with riffles supporting the communities especially rich in rheophilic taxa. The undulated morphology of streambeds enables the exchange of water between river channel and hyporheic zone, crucial to provide oxygen for incubating eggs and larvae of lithophilic fish spawning in river gravels (Boulton 2007).

In modern river engineering there is often a need to construct hydraulic structures which mimic the geometry of natural riffles, while protecting river bed against erosion, directing flow and reducing slope of the channel bed. Such structures are rapid hydraulic structures (called later along that paper RHS) with artificial roughness provided by the stones installed along the slope apron. In some countries such structures are called ramps. Hydrodynamic conditions of the flow conveyed over RHS are similar to those typifying natural riffles. RHS resemble natural riffles also in their high spatial diversity of hydraulic conditions (Radecki-Pawlik et al. 2010), a key factor in creating heterogeneity of physical habitat conditions for benthic invertebrate fauna (Kłonowska-Olejnik, Radecki-Pawlik 2000, Zasępa et al. 2006). The aim of this paper is to analyse chosen hydraulic parameters of a rapid hydraulic structure constructed in a gravel-bed Porębianka Stream, Polish Carpathians.

2 STUDIED STREAM AND FLOW CONDITIONS DURING MEASUREMENTS

Porębianka Stream is a 15.4 km long, 4th-order stream draining a flysch part of the Polish Carpathians. The area of its catchment amounts to 72 km^2, and the width of the channel varies from 1 m at the headwater part of the stream to 140 m at the mouth stretch. Average channel slope equals 56.9‰ (Korpak 2008). Hydrological characteristics of Porębianka were determined on the basis of records at a gauging station located in the middle course of the stream. The present morphology of the Porębianka channel is influenced by check-dams, with channel incision occurring downstream and bed aggradation upstream of the dams (Kościelniak 2004, Korpak 2007). Nowadays, the stream has a single, narrow and winding channel. At the beginning of the twentieth century the stream flowed in a a multi-thread channel. Later its channelization was carried out, with the stream course partitioned by check-dams, weirs and rapid hydraulic structures (ramps) and channel banks reinforced with riprap, gabions and retaining walls (Kościelniak 2004, Korpak et al. 2008). In the lower course of the stream, a grade correction with 25 rapid hydraulic structures (RHS) of high roughness was applied. While reducing channel slope, the structures operate similar to natural riffles and promote accumulation of bed material between them. The paper aims at the analysis of hydraulic parameters in the vicinity of one of the RHS.

Field measurements were made in three series in: April, June and October 2010. At the first series, the measurements were performed during the spring thaw, at the flow of $Q = 2.25\ m^3 \cdot s^{-1}$, higher than mean annual discharge $SSQ = 1.32\ m^3 \cdot s^{-1}$. Between the first and the second series of measurements, a flood with the discharge $Q = 55\ m^3 \cdot s^{-1}$ occurred. During the second series, the discharge amounted to $Q = 2.40\ m^3 \cdot s^{-1}$ and was also higher than the mean. This elevated flow was caused by long-lasting rainfall that occurred in May and at the beginning of June 2010. In October low flows occurred, reflecting low precipitation in the autumn. The discharge equalled then $Q = 1.15\ m^3 \cdot s^{-1}$.

3 METHODOLOGY

One of the rapid hydraulic structures of high roughness in Porębianka Stream was chosen for detailed investigations (Fig. 1). Velocity measurements were carried out upstream and downstream of the structure in the area of its influence and on the ramp itself. Depending on the configuration of channel bed and water stage, measurements were made at 63 measurement points in the first series, at 57 in the second one and at 37 in the third one (Fig. 2).

Figure 1. Studied rapid hydraulic structure (RHS) in Porębianka Stream

Momentary flow velocity was measured with OTT Nautilus 2000 electromagnetic current meter. Based on the measurements, velocity curves were drawn for the velocities over individual measurement points. The momentary flow velocity measurements made it possible to determine the following parameters: depth-averaged velocity, dynamic velocity, Reynolds number (vertical and so called particle one), Froude number, shear stress, Shields parameter.

The value of dynamic velocity was calculated from the velocity profile using the formula (1) (Gordon et al. 2007):

$$v_* = \frac{a}{5.75} \ [\mathrm{m \cdot s^{-1}}] \quad (1)$$

where a is slope of the straight line v = f(h).

The calculated value of the dynamic velocity was used to determine the drag force acting on the channel bed, that is tangential stress, according to the formula (2):

$$\tau = \rho \cdot (v_*)^2 \ [\mathrm{N \cdot m^{-2}}] \quad (2)$$

where $\rho = 1000 \ \mathrm{kg \cdot m^{-3}}$ is water density.

Froude numbers at average and maximum depth were determined according to the formula (3):

$$Fr = \frac{v}{\sqrt{gh}} \ [-] \quad (3)$$

where v is flow velocity $[\mathrm{m \cdot s^{-1}}]$, h is water depth [m], and g is gravitational acceleration $[\mathrm{m \cdot s^{-2}}]$. The obtained values of Fr showed whether the measurement was made in the layer of supercritical flow, subcritical flow and/or critical flow, with the critical Fr value equal 1.

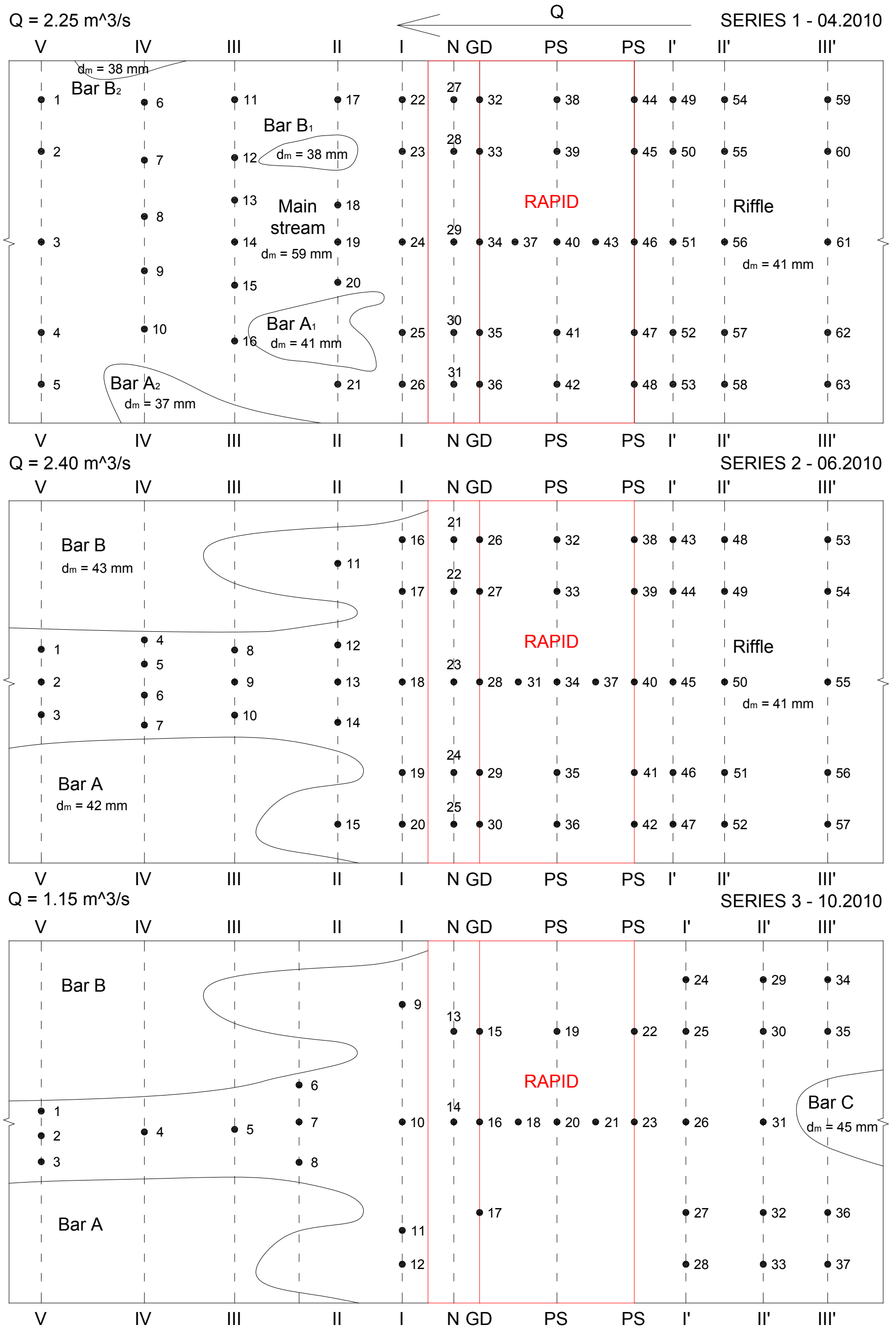

Figure 2. Arrangement of measurement points.

Reynolds numbers were obtained from the formula (4):

$$Re = \frac{v \cdot d}{\nu} \ [-] \qquad (4)$$

where v is flow velocity [m · s^{-1}], d is water depth or the diameter of grains on the bed surface [m], and ν is the coefficient of kinetic viscosity [m^2 · s].

Grain size of the bed material on bars and riffles was also measured. Surface bed material was sampled using the transect Wolman's method (Wolman 1954) and the effective grain sizes were calculated based on the measurements.

4 RESULTS AND DISCUSSION

Table 1 presents the results of hydrodynamic calculations based on data obtained in April 2010. The dynamic velocities and tangential stresses below the rapid hydraulic structure reached the highest values in the cross section "I – I", amounting to 0.029 m · s^{-1} and 0.86 N · m^{-2}, respectively. It reflected high velocity (v_{av} = 0.540 m · s^{-1}) and turbulence of the water flowing down the ramp and out of the energy-dissipating pool of the structure. Moreover, the highest values of the dynamic velocity and shear stresses occurred in the middle part of the channel (points 8, 13, 19). Reynolds numbers indicated that in all the measurement points flow was turbulent. The Froude numbers higher than 1 indicated the occurrence of supercritical flow on the ramp and in the middle part of the energy-dissipating pool.

Table 1: Hydrodynamic parameters (series 1).

Cross-section	**Point number**	**h [m]**	**$v_{śr}$ [m · s^{-1}]**	**v_* [m · s^{-1}]**	**τ [N · m^{-2}]**	**Re [-]**	**Re_* [-]**	**Fr [-]**	**Fr_* [-]**
V – V	1	0.04	0.036	0.007	0.05	1101	1065	0.06	0.005
	2	0.20	0.460	0.009	0.08	70331	1356	0.33	0.007
30 m	3	0.12	0.352	0.003	0.01	32291	544	0.32	0.002
downstream	4	0.18	0.470	0.012	0.14	64674	2472	0.35	0.007
of the pool	5	0.10	0.420	0.007	0.05	10091	1474	0.42	0.004
IV – IV	6	0.05	0.264	0.004	0.02	10091	503	0.38	0.003
	7	0.19	0.710	0.009	0.09	103127	1168	0.52	0.007
22 m	8	0.20	0.450	0.012	0.15	68802	2523	0.32	0.007
downstream	9	0.13	0.402	0.006	0.04	39951	755	0.36	0.005
of the pool	10	0.13	0.396	0.005	0.03	39355	656	0.35	0.004
III – III	11	0.08	0.264	0.005	0.03	16146	691	0.30	0.004
	12	0.05	0.302	0.016	0.26	11543	2019	0.43	0.013
15 m	13	0.27	0.402	0.009	0.08	82975	1869	0.25	0.005
downstream	14	0.22	0.650	0.017	0.29	109319	3575	0.44	0.010
of the pool	15	0.19	0.460	0.003	0.01	66814	343	0.34	0.002
	16	0.05	0.105	0.003	0.01	4013	363	0.15	0.002
II – II	17	0.20	0.212	0.003	0.01	32413	396	0.15	0.002
	18	0.23	0.354	0.014	0.20	62243	2962	0.24	0.009
8 m	19	0.48	0.324	0.018	0.31	118890	3655	0.15	0.011
downstream	20	0.45	0.334	0.011	0.13	114899	2366	0.16	0.007
of the pool	21	0.09	0.044	0.001	0.01	3027	215	0.05	0.001
I – I	22	0.35	0.338	0.009	0.08	90437	1142	0.18	0.007
	23	0.12	0.113	0.007	0.05	10366	903	0.10	0.006
4 m	24	0.53	0.640	0.029	0.86	259307	6115	0.28	0.033
downstream	25	0.19	0.101	0.004	0.02	14670	617	0.07	0.003
of the pool	26	0.09	0.216	0.011	0.13	14861	1653	0.23	0.008
N	27	0.10	0.460	0.008	0.06	35166	2057	0.46	0.004
centre of the	28	0.13	0.400	0.010	0.11	39752	2769	0.35	0.006
energy-dissipating	29	0.10	1.740	0.053	2.85	133017	14276	1.76	0.029
pool	30	0.15	0.206	0.010	0.10	23622	2685	0.17	0.005
	31	0.12	0.530	0.009	0.07	48620	2285	0.49	0.005
GD	32	0.08	0.630	0.003	0.01	38529	805	0.71	0.002
	33	0.04	1.480	0.012	0.14	45256	3215	2.36	0.006
lower concrete sill	34	0.10	2.160	0.040	1.61	165125	10730	2.18	0.022
of the RHS	35	0.03	0.840	0.013	0.18	19265	3564	1.55	0.007
	36	0.03	0.470	0.003	0.01	10779	870	0.87	0.002

Cross-section	Point number	h [m]	$v_{śr}$ [$m \cdot s^{-1}$]	v_* [$m \cdot s^{-1}$]	τ [$N \cdot m^{-2}$]	Re [-]	Re_* [-]	Fr [-]	Fr_* [-]
PS ramp of the RHS	37	0.14	2.380	0.024	0.58	254721	6422	2.03	0.013
	38	0.08	1.150	0.009	0.08	70331	2382	1.30	0.005
	39	0.08	1.140	0.008	0.06	69719	2089	1.29	0.004
	40	0.10	2.450	0.036	1.28	187295	9567	2.47	0.019
	41	0.05	0.254	0.009	0.08	9709	2401	0.36	0.005
	42	0.03	0.950	0.009	0.08	21787	2382	1.75	0.005
	43	0.10	2.270	0.034	1.16	173534	9097	2.29	0.018
GG upper concrete sill of the RHS	44	0.05	0.540	0.014	0.19	41205	3704	0.77	0.007
	45	0.04	0.320	0.007	0.04	7935	1778	0.51	0.004
	46	0.17	0.920	0.022	0.51	119563	6017	0.71	0.012
	47	0.03	0.346	0.003	0.01	9785	870	0.64	0.002
	48	0.07	0.770	0.004	0.01	20641	1010	0.93	0.002
I' – I' 4 m upstream of the RHS	49	0.12	0.360	0.010	0.09	33025	1272	0.33	0.007
	50	0.10	0.212	0.038	0.01	18729	498	0.25	0.005
	51	0.16	0.460	0.008	0.06	56265	1651	0.37	0.005
	52	0.10	0.245	0.004	0.01	18729	524	0.25	0.003
	53	0.12	0.185	0.002	0.005	16971	256	0.17	0.001
II' – II' 8 m upstream of the RHS	54	0.17	0.420	0.011	0.12	54583	1455	0.33	0.009
	55	0.14	0.410	0.011	0.13	43880	1489	0.35	0.009
	56	0.17	0.530	0.017	0.31	68879	3651	0.41	0.011
	57	0.06	0.161	0.005	0.03	7385	688	0.21	0.004
	58	0.16	0.109	0.007	0.04	12499	909	0.09	0.005
III' – III' 15 m upstream of the RHS	59	0.07	0.010	0.001	0.005	535	43	0.01	0.001
	60	0.30	0.500	0.003	0.01	114670	385	0.29	0.002
	61	0.14	0.396	0.010	0.10	42382	1304	0.34	0.008
	62	0.12	0.220	0.0003	0.001	20182	45	0.20	0.001
	63	0.05	0.224	0.005	0.03	8562	707	0.32	0.004

The highest values of depth-averaged velocity were recorded on the ramp of the structure in its central, lowered part, causing concentration of the flow. At points: 34, 37, 40 and 43, the velocities were above 2.00 $m \cdot s^{-1}$ (maximum 2.45 $m \cdot s^{-1}$ at point 40). Also in the energy-dissipating pool and in the marginal parts of the ramp, the velocities were quite high, amounting to 1.00–2.00 $m \cdot s^{-1}$. At point 29 (in the central part of the energy-dissipating pool) the highest values of depth-averaged velocity and bed shear stress were observed, amounting to 0.053 $m \cdot s^{-1}$ and 2.85 $N \cdot m^{-2}$, respectively. Also above, in the central, lowered part of the ramp (points 34, 40, 43), high values of shear stress (1.16–1.61 $N \cdot m^{-2}$) were recorded. Among all the measurement points on the rapid hydraulic structure, the lowest values of tangential stress (0.01–0.51 $N \cdot m^{-2}$) were those recorded on the upper concrete sill. The highest value of Froude number, 2.47, was recorded at point 40 (the middle of the ramp in its central, lowered part). Subcritical flow over the structure occurred at the points situated on the upper sill and at the marginal parts of the lower sill and the energy-dissipating pool.

Table 2: Hydrodynamic parameters (series 2).

Cross-section	Point number	h [m]	$v_{śr}$ [$m \cdot s^{-1}$]	v_* [$m \cdot s^{-1}$]	τ [$N \cdot m^{-2}$]	Re [–]	Re_* [–]	Fr [–]	Fr_* [–]
V – V 30 m downstream	1	0.40	0.780	0.014	0.20	238514	2060	0.39	0.010
	2	0.44	0.760	0.026	0.69	255638	5462	0.37	0.016
	3	0.30	0.530	0.031	0.94	121550	4350	0.31	0.023
IV – IV 22 m downstream of the pool	4	0.05	0.264	0.028	0.77	10091	4090	0.38	0.020
	5	0.50	0.780	0.024	0.58	298142	5005	0.35	0.015
	6	0.28	0.570	0.017	0.28	122009	3513	0.34	0.010
	7	0.10	0.248	0.008	0.06	18959	1085	0.25	0.006
III – III 15 m downstream	8	0.50	0.430	0.021	0.43	164361	3063	0.19	0.015
	9	0.76	0.520	0.019	0.37	302118	4029	0.19	0.012
	10	0.36	0.390	0.027	0.73	107331	3840	0.21	0.020
II – II 8 m downstream of the pool	11	0.44	0.045	0.002	0.005	15136	250	0.02	0.002
	12	0.40	0.270	0.020	0.41	82562	4218	0.14	0.012
	13	0.83	0.960	0.026	0.74	609128	12083	0.34	0.035
	14	0.12	0.158	0.006	0.03	14494	1234	0.15	0.004
	15	0.50	0.074	0.011	0.13	28285	1261	0.03	0.009

Cross-section	Point number	h [m]	$v_{śr}$ [m · s^{-1}]	v_* [m · s^{-1}]	τ [N · m^{-2}]	Re [–]	Re_* [–]	Fr [–]	Fr_* [–]
I – I	16	1.05	0.010	0.001	0.001	8027	131	0.01	0.001
	17	0.16	0.128	0.008	0.06	15656	901	0.10	0.007
4 m	18	0.60	1.120	0.030	0.87	513722	6167	0.46	0.018
downstream	19	0.09	0.042	0.006	0.04	2890	698	0.04	0.005
of the pool	20	0.94	0.148	0.007	0.04	106353	737	0.05	0.005
N	21	0.10	0.770	0.016	0.27	58864	4388	0.78	0.009
centre of the	22	0.14	0.650	0.028	0.81	69567	7594	0.55	0.015
energy-dissipating	23	0.18	2.100	0.050	2.48	288969	13313	1.58	0.027
pool	24	0.15	0.330	0.009	0.07	37841	2308	0.27	0.005
	25	0.05	0.780	0.015	0.23	29814	4081	1.11	0.008
GD	26	0.08	0.770	0.006	0.04	47091	1661	0.87	0.003
	27	0.06	1.420	0.013	0.16	65133	3402	1.85	0.007
lower concrete sill	28	0.12	2.860	0.069	4.82	262365	18585	2.64	0.037
of the RHS	29	0.03	0.680	0.011	0.11	15595	2834	1.25	0.006
	30	0.06	0.860	0.012	0.15	39447	3257	1.12	0.007
PS	31	0.12	2.050	0.038	1.45	94030	10181	2.67	0.021
	32	0.08	0.960	0.013	0.16	58711	3360	1.08	0.007
ramp	33	0.08	1.140	0.040	1.57	69719	10605	1.29	0.021
of the RHS	34	0.10	1.980	0.051	2.59	105955	13615	2.39	0.027
	35	0.05	1.040	0.044	1.97	39752	11871	1.48	0.024
	36	0.05	0.930	0.025	0.60	35548	6566	1.33	0.013
	37	0.15	1.560	0.045	2.04	178885	12071	1.29	0.024
GG	38	0.08	0.870	0.014	0.20	53207	3820	0.98	0.008
	39	0.06	0.660	0.007	0.04	30273	1778	0.89	0.004
upper concrete sill	40	0.20	1.070	0.034	1.12	163596	8967	0.76	0.018
of the RHS	41	0.05	0.600	0.012	0.15	22934	3267	0.86	0.007
	42	0.05	0.570	0.007	0.06	21787	2006	0.81	0.004
I' – I'	43	0.21	0.400	0.024	0.56	64215	4954	0.28	0.015
	44	0.14	0.169	0.008	0.06	18087	1582	0.14	0.005
4 m	45	0.32	0.690	0.018	0.31	168794	3677	0.39	0.011
upstream	46	0.14	0.368	0.015	0.23	39385	3147	0.31	0.009
of the RHS	47	0.12	0.164	0.009	0.08	15045	1898	0.15	0.006
II' – II'	48	0.24	0.540	0.025	0.62	99075	5201	0.35	0.015
	49	0.10	0.330	0.012	0.13	25227	2425	0.33	0.007
8 m	50	0.20	0.530	0.015	0.23	81034	3194	0.38	0.009
upstream	51	0.15	0.246	0.012	0.15	28209	2515	0.20	0.007
of the RHS	52	0.12	0.152	0.008	0.06	13944	1670	0.14	0.005
III' – III'	53	0.28	0.680	0.012	0.14	145555	1592	0.41	0.009
	54	0.11	0.400	0.038	1.45	33637	5193	0.39	0.029
15 m	55	0.20	0.600	0.023	0.51	91736	4729	0.43	0.014
upstream	56	0.16	0.264	0.020	0.40	32291	2722	0.21	0.015
of the RHS	57	0.12	0.344	0.019	0.36	31557	2594	0.32	0.014

Table 2 presents hydrodynamic parameters determined during the second series of measurements in June 2010. During the flood in May 2010, the channel changed its geometry. Directly downstream of the RHS (cross-section "I – I"), pools formed at both sides of the channel (0.94 m and 1.05 m deep), with low values of depth-averaged velocity (0.148 m · s^{-1} and 0.010 m · s^{-1} for the right and left pool, respectively) and tangential stress (0.001 – 0.005 N · m^{-2} for the right pool and 0.04 – 0.13 N · m^{-2} for the left one). Downstream of the structure, dynamic velocity attained the highest values of the 0.026–0.031 m · s^{-1} and shear stress those of 0.69 – 0.94 N · m^{-2}. Closer to the banks, where the flow velocity was lower, the values of shear stress were lower than in the middle part of the channel (0.13 – 0.62 N · m^{-2}). Turbulent and subcritical flow occurred at all investigated points.

The highest values of depth-averaged velocity, 2.86 m · s^{-1}, and shear stress, 4.82 N · m^{-2}, were recorded on the lower sill (point 28). At the majority of the remaining points, high values of tangential stress occurred as well (2.48 at point 23 in the energy-dissipating pool, 1.45, 1.57, 2.59, 1.97 and 2.04 N · m^{-2} respectively at points 31, 33, 34, 35, 37 on the ramp and 1.12 N · m^{-2} at point 40 on the upper sill). The high values of this parameter are connected with the high values of depth-averaged and dynamic velocity, and the large water turbulence. Such conditions on the RHS were created pools to the lowering applied in order to concentrate the stream. In the energy-dissipating pool, supercritical flow occurred only at two points (23, 25), at the remaining ones subcritical flow occurred.

Upstream of the structure, depth-average velocity varied between 0.164 and 0.690 $m \cdot s^{-1}$, dynamic velocity was in the range of 0.008 –0.038 $m \cdot s^{-1}$, and tangential stress – 0.06 – 0.62 $N \cdot m^{-2}$. Here, the highest value of the stress, 1.45 $N \cdot m^{-2}$, was recorded at point 54.

The whole set of hydrodynamic data collected during the third series of measurements is not presented in the paper but their analysis is presented below. Directly downstream of the RHS (cross-section "I – I"), further scour of the pools occurred between the second and the third series of measurements. In spite of the low water level, their depth increased (right pool) or remained the same (left pool) in comparison with the series 2. Now the smallest values of dynamic velocity and tangential stress occurred at the pools, and they equalled 0.001 $m \cdot s^{-1}$ and 0.001 $N \cdot m^{-2}$, respectively, for both pools. At the remaining points downstream of the structure, the values of tangential stress were lower than during the second series, which is connected with the lower discharge and and dynamic velocity. Here, the highest values of shear stress (0.38 $N \cdot m^{-2}$ at point 10 and 0.32 $N \cdot m^{-2}$ at point 4) were recorded in the thalweg. Turbulent flow occurred at all points except the pools in which transitional flow was observed. At all points below the structure, the Froude number was below 1, so the subcritical flow occurred. The highest depth-averaged velocity was recorded at point 18 (2.16 $m \cdot s^{-1}$) and point 20 (2.23 $m \cdot s^{-1}$). The highest dynamic velocity and tangential stress occurred on the lower sill and in the central, lowered part of the ramp, amounting to 0.062 $m \cdot s^{-1}$ and 3.90 $N \cdot m^{-2}$, respectively. At the remaining measurement points, the stress values varied between 0.21 and 0.91 $N \cdot m^{-2}$. The exception was point 24 in the energy-dissipating pool, where the value of this parameter equalled 0.03 $N \cdot m^{-2}$. The Reynolds number showed the occurrence of turbulent flow. Supercritical flow occurred almost on the whole ramp and the highest value of Froude number, 3.18, was recorded at point 20.

The values of Froude number, Reynolds number and flow velocity measured on the structure are very important for evaluation of the possibilities of migration of aquatic animals through the ramp. The ecological requirements that must be fulfilled by fish passes and similar structures, such as RHS, are formulated by DVWK (2002). The obtained data indicate that the RHS constructed on Porębianka Stream meets these requirements.

5 CONCLUSIONS

1 Hydrodynamic parameters in the area of the rapid hydraulic structures which mimic natural riffles in gravel-bed rivers depend closely on the location of the measurement point in relation to the individual parts of the structure.
2 Hydrodynamic conditions in the areas of rapid hydraulic structures are highly diversified, which increases heterogeneity of the habitat conditions for benthic invertebrate fauna.
3 The highest velocities were observed on the slope apron of the RHS in the place of flow concentration. At the same time, it is the place where fish and invertebrate can migrate along the structure under low-flow conditions.
4 The maximum, medium and dynamic velocities recorded upstream and downstream of the structure are similar, which shows the proper functioning of the RHS.
5 The values of the shear stress depend directly on flow velocity and water turbulence as well as on the dynamic velocity in all measured places of the investigated RHS.
6 Rapid hydraulic structures (sometimes called ramps) operate as low transversal structures mimicking natural riffles, and thus they conform with the requirements of the Water Framework Directive of the EU.

NOTATION

v	flow velocity [$m \cdot s^{-1}$]
h	water depth [m]
g	gravitational acceleration [$m \cdot s^{-2}$]
d	diameter of the grains on the channel bed [m]
ν	coefficient of kinetic viscosity [$m^2 \cdot s$]
v_{sr}	depth-averaged flow velocity [$m \cdot s^{-1}$]
Re*	particle Reynolds number
Fr*	particle Froude number

REFERENCES

Boulton, A.J. (2007). Hyporheic rehabilitation in rivers: restoring vertical connectivity. Freshwater Biology, 52, 632-650.

DVWK (2002). Fish passes – Design, dimensions and monitoring. Published by the Food and Agriculture Organization of the United Nations in arrangement with Deutscher Verband für Wasserwirtschaft und Kulturbau e.V. (DVWK), Rome, 2002.

Gregory, K.J., Gurnell, A.M., Hill, C.T., Tooth, S. (1994). Stability of the pool-riffle sequence in changing river channels. Regulated Rivers: Research and Management, 9, 35-43.

Gordon, N.D., McMahon, T.A., Finlayson, B.L., Gippel, C.J., Nathan, R.J. (2007). Stream Hydrology – an Introduction for Ecologists. Wiley and Sons. London.

Keller, E.A. (1971). Areal sorting of bed-load material: The hypothesis of velocity reversal. Bulletin of the Geological Society of America, 82, 753-756.

Kłonowska-Olejnik, M., Radecki-Pawlik, A. (2000). Zróżnicowanie mikrosiedliskowe makrobezkręgowców dennych w obrębie łach korytowych potoku górskiego o dnie żwirowym. XVIII Zjazd Hydrobiologów Polskich. Białystok.

Korpak, J. (2007). Morfologiczna rola budowli regulacyjnych w górskich systemach fluwialnych. Doctoral Thesis. Kraków. Manuscript.

Korpak, J. (2008). Rola maksymalnych wezbrań w funkcjonowaniu systemów uregulowanych koryt górskich. Landform Analysis. 8, 41-44.

Korpak, J., Krzemień, K., Radecki-Pawlik, A. (2008). Wpływ czynników antropogenicznych na zmiany koryt cieków karpackich. Infrastruktura i Ekologia Terenów Wiejskich 4, Kraków.

Kościelniak J. (2004). Zmiany funkcjonowania górskich systemów korytowych w wyniku przeprowadzonych regulacji hydrotechnicznych. Prace Geograficzne, 200.

Milne, J.A. (1982). Bed-material size and the riffle-pool sequence. Sedimentology, 29, 267-278.

Montgomery, D.R., Buffington, J.M. (1997). Channel-reach morphology in mountain drainage basins. Geological Society of America Bulletin, 109, 596-611.

Pastuchová, Z., Lehotský, M., Grešková, A. (2008). Influence of morphodynamic habitat structure on invertebrate communities (Ephemeroptera, Plecoptera and Trichoptera). Biologia, 63, 720-729.

Radecki-Pawlik A. (2002). The velocity-reversal hypothesis – implications for a mountainous stream bed morphology. Electronic Journal of Polish Agricultural Universities, 5(2).

Radecki-Pawlik A., Świderska K., Plesiński K. (2010). Zróżnicowanie parametrów hydraulicznych w rejonie bystrzy o zwiększonej szorstkości. Infrastruktura i Ekologia Terenów Wiejskich, 1, 25-38.

Teisseyre, A.K. (1984). The River Bóbr in the Błażkowa study reach (central Sudetes): A study in fluvial processes and fluvial sedimentology. Geologia Sudetica, 19(1), 8-65.

Wolman, M.G. (1954). A method of sampling coarse river-bed material. Transactions, American Geophysical Union, 35(6), 951-956.

Zasępa, P., Radecki-Pawlik, A., Kłonowska-Olejnik, M., Przybyła, K. (2006). Zróżnicowanie mikrosiedlisk makrobezkręgowców dennych w obrębie łachy bocznej potoku górskiego. Infrastruktura i Ekologia Terenów Wiejskich, 2(2), 5-16.